WFUMB 2023
YOUNG INVESTIGATOR ABSTRACT AFSUMB

An Unsupervised Deep Beamformer for High-Quality Ultrafast Ultrasound Imaging

Hyunwoo Cho[1], Jinbum Kang[2], Yangmo Yoo[1,3]

[1]*Department of Electronic Engineering, Sogang University, Seoul, Korea*

[2]*Department of Bioengineering, University of Washington, Seattle, WA 98105, United States*

[3]*Department of Biomedical Engineering, Sogang University, Seoul, Korea*

ABSTRACT

Introduction

Ultrafast imaging in medical ultrasound is becoming an important reconstruction method with high frame rates and new clinical applications such as shear wave elastography and microvascular imaging. However, the unfocused waves lead to low-quality images and required additional compounding to mitigate the image degradation. Recently, deep learning (DL) based image reconstruction methods showed great potential for high-quality ultrafast imaging and the conventional methods mostly used supervised learning approaches. However, acquiring high-quality ground-truth data in medical ultrasound for supervised learning is not only extremely challenging but also limited the performance of DL models.

Aims & Methods

To address this critical issue, this study proposes a new unsupervised learning approach for high-quality ultrafast ultrasound imaging. Unlike conventional methods that train DL models using supervised learning with imperfect ground-truth data, our method employs unsupervised learning using signal coherence with a unique loss function. Because the trained DL models aim to maximize signal coherence, our model minimizes unnecessary secondary lobes and noise, resulting in improved spatial and contrast resolution. Additionally, our trained model is a universal beamformer since it operates on complex baseband signals, making it suitable for various clinical applications such as vector flow imaging and microvascular imaging.

Results

To assess the performance of the proposed method (DL-DCL), traditional beamformers (i.e., DAS and DMAS) and other DL-based methods (i.e., supervised learning method (SP) and generative adversarial network (GAN)) were compared. Our proposed method showed far improved results in spatial and contrast resolution, and the results were even comparable to the compounded image (75-PWs) with a single PW. Also, our method surpassed the conventional SP and GAN models without the generation of ground-truth data.

Conclusion

These results demonstrated that the proposed unsupervised learning approach can overcome the limitations of conventional DL methods based on supervised learning, and it also showed great potential in clinical settings with minimal artifacts.

Keywords: Ultrafast ultrasound imaging, adaptive beamforming, deep learning, unsupervised learning.

Materials

Figure 1. Illustration of plane wave imaging for ultrafast ultrasound imaging. Plane wave imaging insonifies the entire imaging field to enable high frame rates (left). The degraded imaging quality can be improved by coherent compounding (right), but compounding using multiple transmissions sacrifices frame rates.

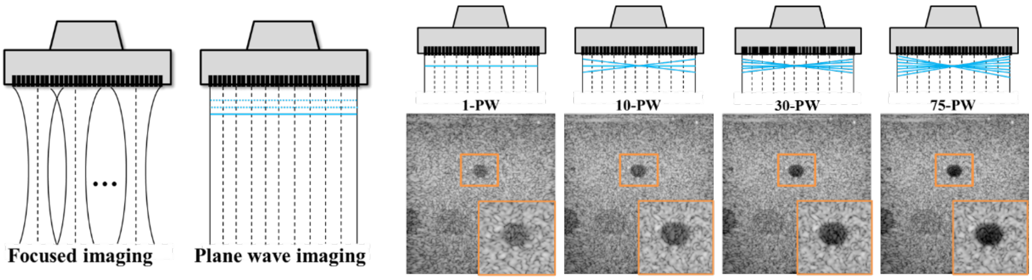

Figure 2. Schematic representation of the proposed unsupervised deep learning framework. (a) During the training phase, the deep learning model is trained using the signal coherence between the steered plane waves. (b) After training, the trained model can be utilized as a beamforming module to enhance the imaging quality of a single plane wave transmission.

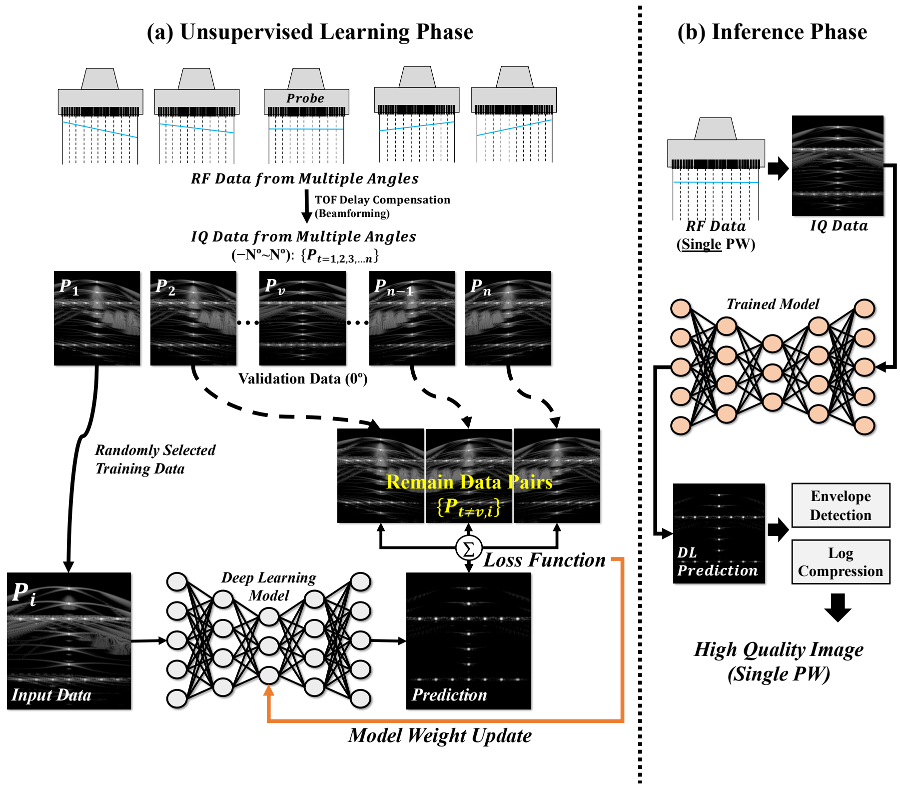

Figure 3. Qualitative and quantitative assessment of experiments with wire-target and cyst-target phantoms.

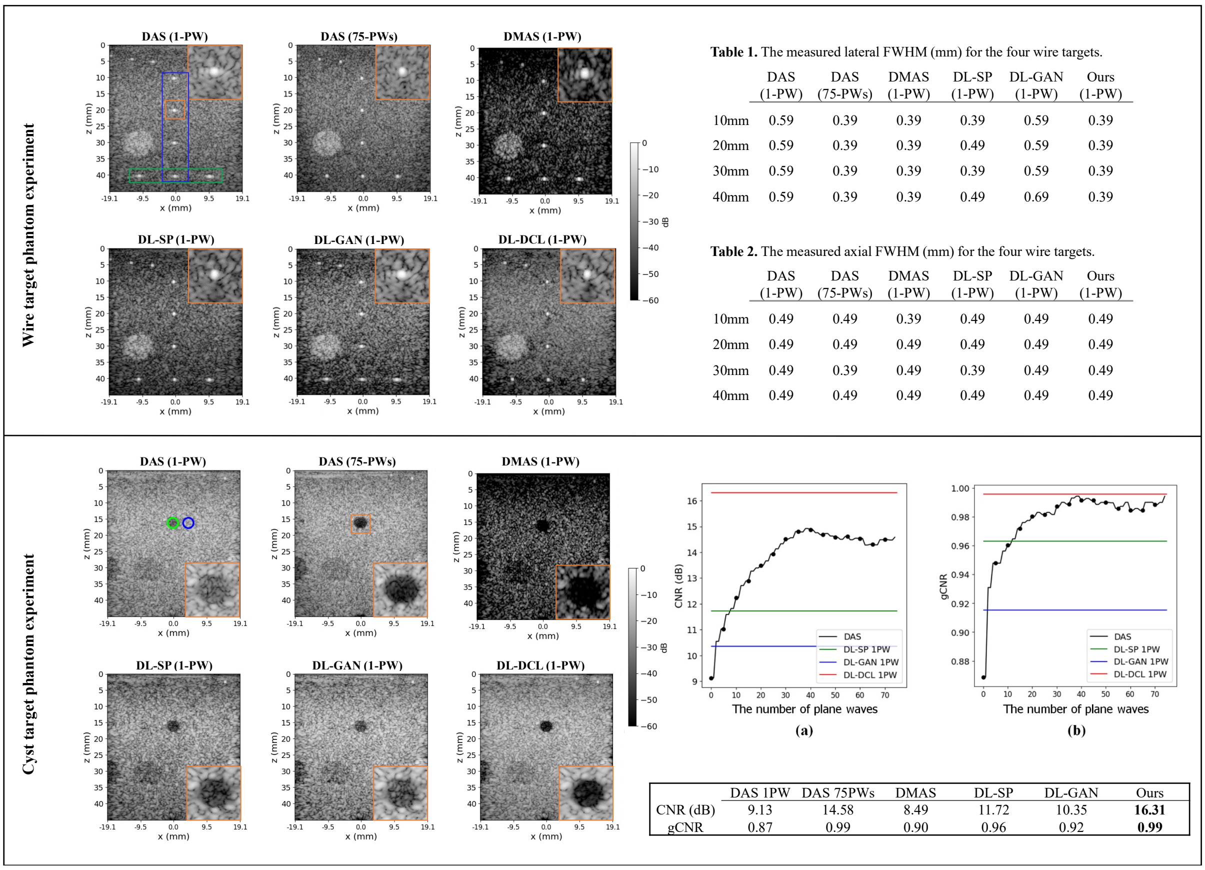

Table 1. The measured lateral FWHM (mm) for the four wire targets.

	DAS (1-PW)	DAS (75-PWs)	DMAS (1-PW)	DL-SP (1-PW)	DL-GAN (1-PW)	Ours (1-PW)
10mm	0.59	0.39	0.39	0.39	0.59	0.39
20mm	0.59	0.39	0.39	0.49	0.59	0.39
30mm	0.59	0.39	0.39	0.39	0.59	0.39
40mm	0.59	0.39	0.39	0.49	0.69	0.39

Table 2. The measured axial FWHM (mm) for the four wire targets.

	DAS (1-PW)	DAS (75-PWs)	DMAS (1-PW)	DL-SP (1-PW)	DL-GAN (1-PW)	Ours (1-PW)
10mm	0.49	0.49	0.39	0.49	0.49	0.49
20mm	0.49	0.49	0.49	0.49	0.49	0.49
30mm	0.49	0.39	0.49	0.39	0.49	0.49
40mm	0.49	0.49	0.49	0.49	0.49	0.49

	DAS 1PW	DAS 75PWs	DMAS	DL-SP	DL-GAN	Ours
CNR (dB)	9.13	14.58	8.49	11.72	10.35	**16.31**
gCNR	0.87	0.99	0.90	0.96	0.92	**0.99**

Figure 4. Qualitative and quantitative assessment of experiments using two publicly available *in-vivo* images.

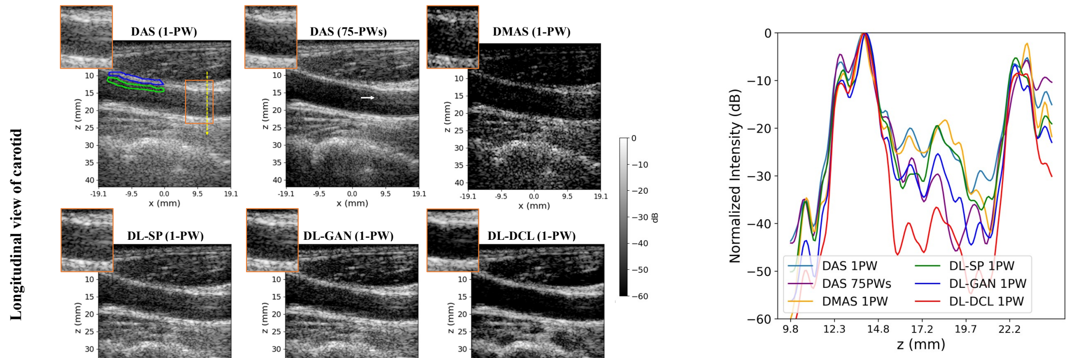

	DAS 1PW	DAS 75PWs	DMAS	DL-SP	DL-GAN	Ours
CNR (dB)	14.60	16.12	11.31	14.87	16.02	18.63
gCNR	0.99	0.99	0.95	0.99	0.99	0.99

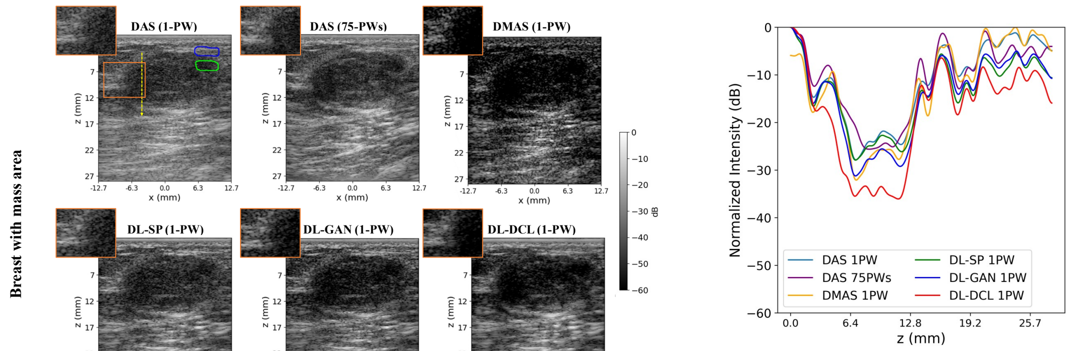

	DAS 1PW	DAS 75PWs	DMAS	DL-SP	DL-GAN	Ours
CNR (dB)	12.17	13.15	11.59	12.40	12.54	13.79
gCNR	0.97	0.98	0.99	0.99	0.99	0.99